2014

Hydrogeologic Investigations of Pavement Subsidence in the Cumberland Gap Tunnel

James S. Dinger
University of Kentucky, james.dinger@uky.edu

James C. Currens
University of Kentucky, currens@uky.edu

Junfeng Zhu
University of Kentucky, junfeng.zhu@uky.edu

Steven E. Webb
University of Kentucky, steven.webb@uky.edu

Brad W. Rister
University of Kentucky, brad.rister@uky.edu

See next page for additional authors

Authors
James S. Dinger, James C. Currens, Junfeng Zhu, Steven E. Webb, Brad W. Rister, R. C. Graves, David L. Allen, and Tim C. Scully

Kentucky Geological Survey
James C. Cobb, State Geologist and Director
University of Kentucky, Lexington

Hydrogeologic Investigations of Pavement Subsidence in the Cumberland Gap Tunnel

James S. Dinger, James C. Currens,
Junfeng Zhu, Steven E. Webb, Brad W. Rister,
R.C. Graves, David L. Allen, and Tim C. Scully

Report of Investigations 27 https://doi.org/10.13023/kgs.ri27.12 Series XII, 2014

In memory of Anita Spears, a KGS employee, conscientious student, colleague, friend, caver, and mom. Born September 16, 1967, and passed away December 28, 2008.

Kentucky Geological Survey
James C. Cobb, State Geologist and Director
University of Kentucky, Lexington

Hydrogeologic Investigations of Pavement Subsidence in the Cumberland Gap Tunnel

James S. Dinger, James C. Currens, Junfeng Zhu, Steven E. Webb, Brad W. Rister, R.C. Graves, David L. Allen, and Tim C. Scully

Report of Investigations 27 https://doi.org/10.13023/kgs.ri27.12 Series XII, 2014

Our Mission

Our mission is to increase knowledge and understanding of the mineral, energy, and water resources, geologic hazards, and geology of Kentucky for the benefit of the Commonwealth and Nation.

Earth Resources—Our Common Wealth

www.uky.edu/kgs

Technical Level

General **Intermediate** **Technical**

ISSN 0075-5591

Contents

Figures

Tables

Hydrogeologic Investigations of Pavement Subsidence in the Cumberland Gap Tunnel

James S. Dinger[1], James C. Currens[1], Junfeng Zhu[1], Steven E. Webb[1]
and
Brad W. Rister[2], R.C. Graves[2], David L. Allen[2], and Tim C. Scully[2]

Abstract

Cumberland Gap Tunnel was constructed under Cumberland Gap National Historical Park in 1996 to improve transportation on a segment of U.S. 25E, connecting Kentucky and Tennessee and restoring Cumberland Gap to its historical appearance.

The concrete pavement in the tunnel started to subside in 2001. Ground penetrating radar surveys revealed voids in many areas of the limestone roadbed aggregate beneath the pavement. To investigate possible hydrogeologic processes that may have caused favorable conditions for voids to form in the aggregate, we studied geology, groundwater flow, and groundwater chemistry in the tunnel using a variety of methods, including bore drilling, packer test, dye tracing, groundwater- and surface-flow monitoring, water-chemistry modeling, and an aggregate dissolution experiment.

The study revealed that the aggregate receives a large volume of groundwater from much of the bedrock invert, but the flow velocity is too slow to transport small particles out of the aggregate. Calcite saturation indices calculated from water-chemistry data suggest that the groundwater was capable of continuously dissolving calcite, the primary mineral in the limestone aggregate. Water samples taken during different flow conditions indicate that groundwater under high-flow conditions could dissolve calcite more quickly than groundwater under low-flow conditions. The dissolution experiment showed that all the limestone aggregate placed beneath the roadbed and in contact with groundwater lost mass; the highest mass loss was 3.4 percent during a 178-day period. The experiment also suggested that water with higher calcite-dissolving potential removed limestone mass quicker than water with low calcite-dissolving potential.

We recommend that the limestone aggregate be replaced with noncarbonate aggregate, such as granite, to prevent dissolution and future road subsidence.

Introduction

On October 18, 1996, a segment of U.S. 25E from Middlesboro, Ky., to Harrogate, Tenn., was relocated into a newly constructed tunnel beneath Cumberland Mountain, to improve transportation efficiency and safety as well as help restore Cumberland Gap to its appearance when Daniel Boone brought the first settlers to Kentucky in the mid-

[1]Kentucky Geological Survey, University of Kentucky
[2]Kentucky Transportation Center, University of Kentucky

1770's. The tunnel is approximately 4,150 ft long and consists of two bores, one southbound and one northbound, each having two lanes for traffic. Approximately 22,500 vehicles pass through the two bores each day. In 2001, multiple areas of the highway pavement in the southbound bore began to subside. In 2005, the Kentucky Transportation Center at the University of Kentucky conducted ground penetrating radar surveys in the tunnel, and the surveys indicated multiple voids beneath the concrete pavement in both bores (Rister, 2005). Some of the void areas spanned both lanes. Pavement coreholes and lithologic core borings revealed voids up to 40 in. deep. From 2006 to 2012, the Kentucky Geological Survey at the University of Kentucky teamed with the Transportation Center to conduct hydrogeologic investigations in the tunnel to assess physical or chemical processes that might contribute to the formation of the voids and subsequent subsidence.

Project Location

The Cumberland Gap Tunnel is in the Middlesboro South 7.5-minute quadrangle (Fig. 1). The tunnel extends beneath Cumberland Mountain between Kentucky and Tennessee and replaced the segment of U.S. 25E that crossed the Cumberland Gap National Historic Park overland. Coordinates of the tunnel are approximately 37°10′ N latitude and 83°41′ W longitude.

General Geology

The stratigraphic section pierced by the tunnel consists primarily of carbonate rocks of Late

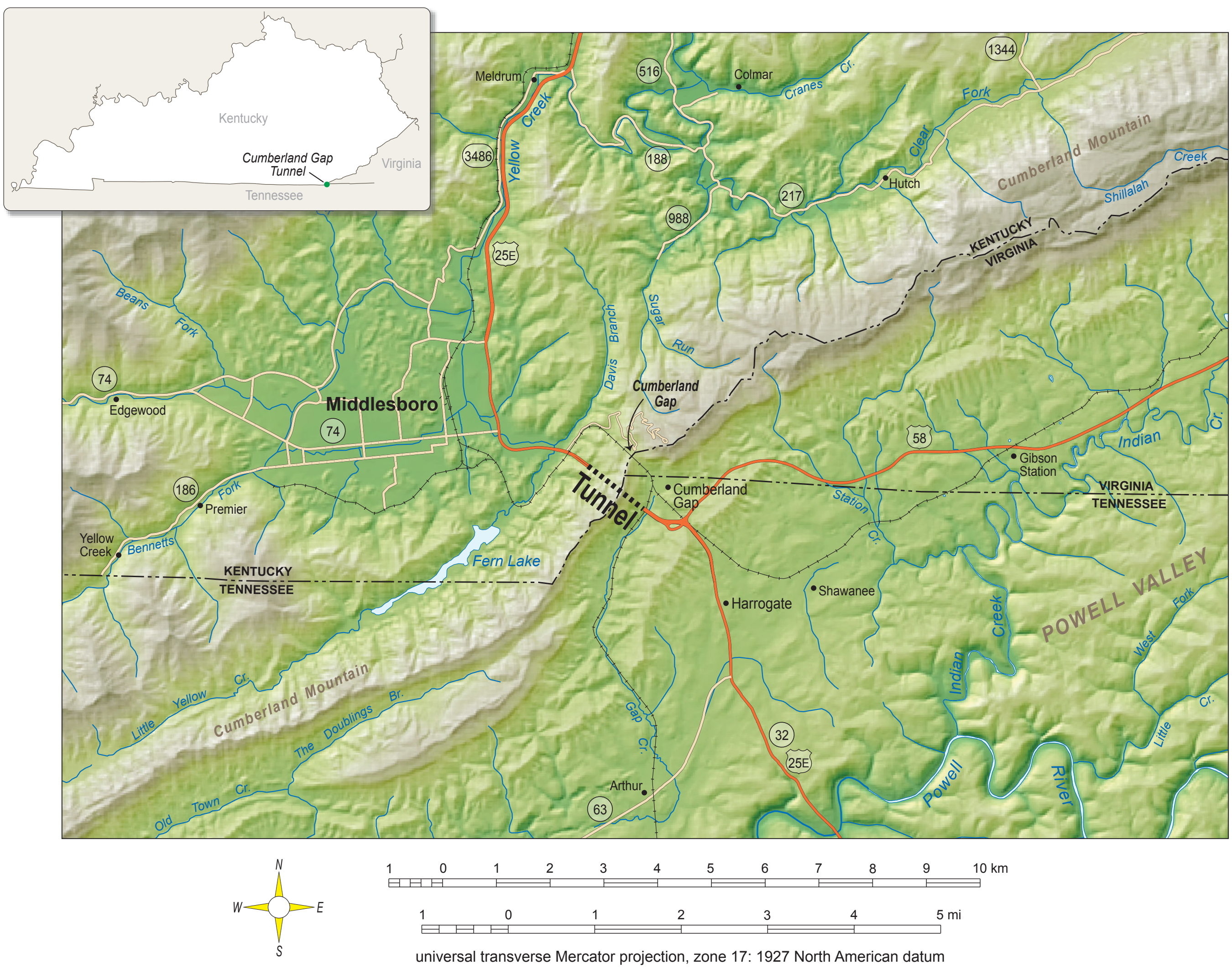

Figure 1. Location of the Cumberland Gap Tunnel.

Silurian and Mississippian age and clastic strata of Early Pennsylvanian age. Cumberland Mountain is on the southeastern margin of the structural wedge of the Pine Mountain Thrust Sheet. The strata are tilted approximately 40° to the northwest and there are no major faults. The tunnel transects the strata at almost 90° (Fig. 2). The stratigraphy and structure at the Cumberland Gap Tunnel have been described in precise detail by Golder Associates (1987) and Vanover (1989). Earlier work by Englund (1964) set the framework on which the other reports are based.

Roadbed Subsidence Problems

The pavement subsidence was first noticed in 2001 in the southbound tunnel between stations 119.50 and 140.50. Stations represent distances in hundredths of feet from the beginning of a road project. For the Cumberland Gap Tunnel, the starting location is the northwest (Kentucky) side outside the tunnel. The magnitude of the pavement settlement was approximately 1 to 3 in. An expansive foam material was installed beneath the subsiding pavement to lift the pavement back to the proper elevation, but the foam failed to lift the pavement. In 2005, the Transportation Center conducted ground penetrating radar surveys and found voids in the roadbed aggregate backfill material beneath the pavement in both bores. The aggregate consists of crushed limestone of 0.5 to 1 in. diameter, commonly referred to as No. 57 aggregate. The voids ranged in diameter from 2 to 40 in. Some voids spanned two lanes and extended up to 70 ft in length. The pavement was still in service because of reinforcing steel placed inside the concrete, but engineering recommendations state that concrete pavement can only span voids with diameters less than 6 ft before the pavement is permanently deformed.

Previous Hydrogeologic Investigations

Geotechnical investigations prior to the design phase of the tunnel project found that the groundwater flow would converge toward the aggregate base of the roadway (Golder Associates, 1987). Inflows between stations 131.50 and 142.20 (Middlesboro Formation) ranged from 700 gal/min to between 40 and 100 gal/min. Other major inflows between stations 118.50 and 129.30 ranged from 1,100 gal/min to 270 to 360 gal/min. The majority of the inflow came from a single location at station 123.20, initially at 800 gal/min and leveling off at 100 gal/min.

Golder Associates (1987) was concerned with the stability of the crown and sidewalls in the traffic tunnel in response to hydrostatic pressure, particularly in the coarser-grained sandstone units. Slaking of friable or deformable clay shale was considered a potentially significant but solvable condition during construction. Golder Associates (1987) also evaluated disposal of the large volume of water discharged from the bedrock and karst aquifers, and suggested possible designs for disposal. They recommended an underdrain system for the

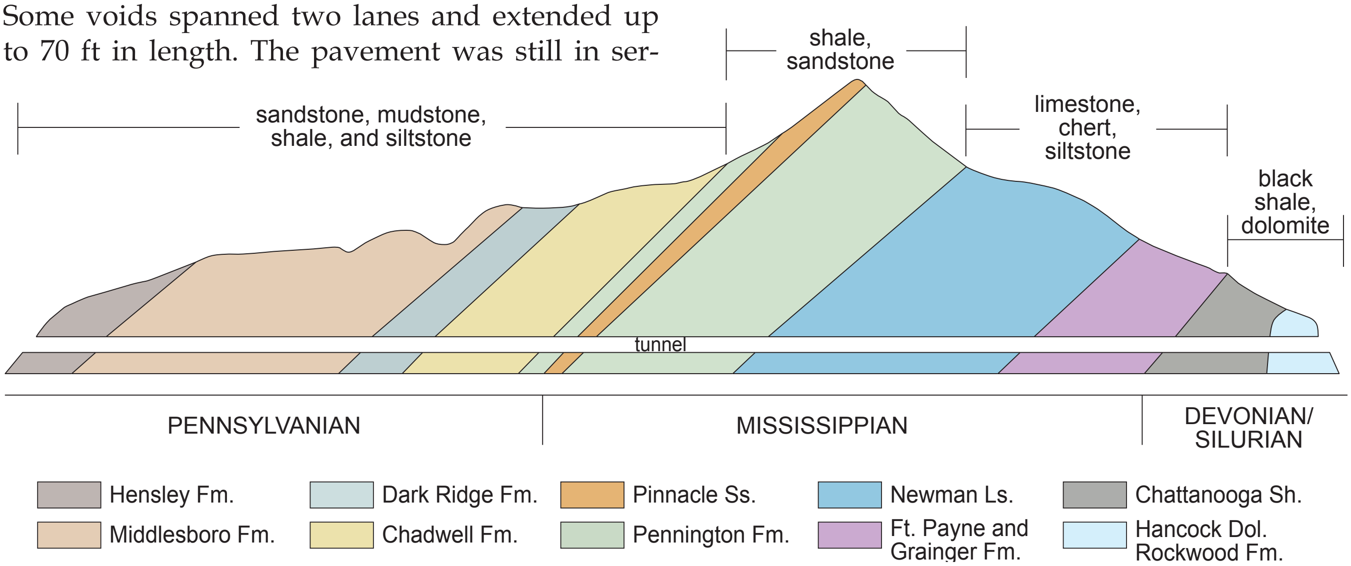

Figure 2. Geologic cross section of the Cumberland Gap Tunnel.

groundwater inflow to prevent preconstruction head conditions being reestablished, which could cause the tunnel lining to fail. They felt that deposition of ferrous precipitates had the potential to block the groundwater drains, but did not discuss the potential for loosened silt or clay material to be transported by groundwater.

Golder Associates' (1987) geotechnical investigation also showed that the Mississippian limestone sections were highly weathered, containing small cavities and larger caverns. A locally extensive cave system was discovered between stations 146.00 and 151.00. Golder Associates (1987) predicted major sustained inflow in the vicinity of the cave system, which would increase substantially during storms.

Hydrogeologic Investigations

First Phase: Core Drilling, Lithologic Logging, Packer Tests, and Dye Tracing

The ground penetrating radar surveys conducted in 2005 by the Kentucky Transportation Center indicated that the voids in the roadbed aggregate were beneath the concrete pavement in at least six nearly juxtaposed locations in each bore. The proximity of the subsidence in the two parallel bores indicates that discrete geologic strata or structure are involved. Documentation of hydrogeotechnical conditions encountered in the initial pilot tunnel and during the construction of the two highway bores indicated local zones of high groundwater discharge, mudstone strata, major joints and minor faults, or combinations of all in the subsidence zones. An initial hypothesis was that convergence of groundwater flow and resulting increased velocity in the subsidence zones, into and through the drainage field in the aggregate, might be physically eroding the aggregate or creating upwelling conditions into which aggregate was sinking. Either or both of these processes would undermine support for and lead to subsidence of the overlying pavement. To test the hypothesis, the first phase focused on the strata in which the voids appeared and on groundwater flow in the vicinity. During this phase, lithologic logging, packer tests, and dye tracing were conducted.

Core Drilling and Lithologic Logging. In June 2006, a technical group from the Federal Highway Administration drilled five core boreholes, CB-1 through CB-5, into the bedrock in the southbound bore. Borings were preferentially located in and around roadbed aggregate void zones previously defined by the 2005 ground penetrating radar study. Locations and characteristics of the cores are shown in Table 1.

A downhole camera was lowered down two coreholes (CB-3 and CB-4). These coreholes had voids, soft zones, and poor core recovery, described in the lithologic logs obtained during the coring process. Video logs were viewed and correlated to the lithologic descriptions. Of particular interest were the fractures, wash-out and void zones, and movement of rock particles in the borehole in response to groundwater moving through the voids.

Bhate Engineering Corp.–Transportation Division (1992) developed cross sections using corehole logs, video logs, and maps made during tunnel excavation. All references in the Bhate Engineering report to station numbers should be regarded as estimates. Mapped features were projected to the tunnel invert unless otherwise noted. Groundwater discharges were estimates by Bhate Engineering (1992) during tunnel construction. All depths were measured from the top of the roadway pavement. In the cross sections (Figs. 3–5), the first encounter of bedrock at the tunnel invert is labeled "rock." Thicknesses of distinctive lithologic units as defined by Bhate Engineering (1992) vary from the

Table 1. General characteristics of core borings in the southbound tube, completed in June 2006.

Core Boring	*CB-1*	*CB-2*	*CB-3*	*CB-4*	*CB-5*
Station Number	122.55	138.60	138.90	122.85	129.00
Ground Penetrating Radar Void Stations	122.00–123.35	138.70–139.80	122.00–139.80	122.00–123.35	128.34–129.36
Depth (ft)	44.6	39.7	29.5	44.4	49.7
Video Log	no	no	yes	yes	no

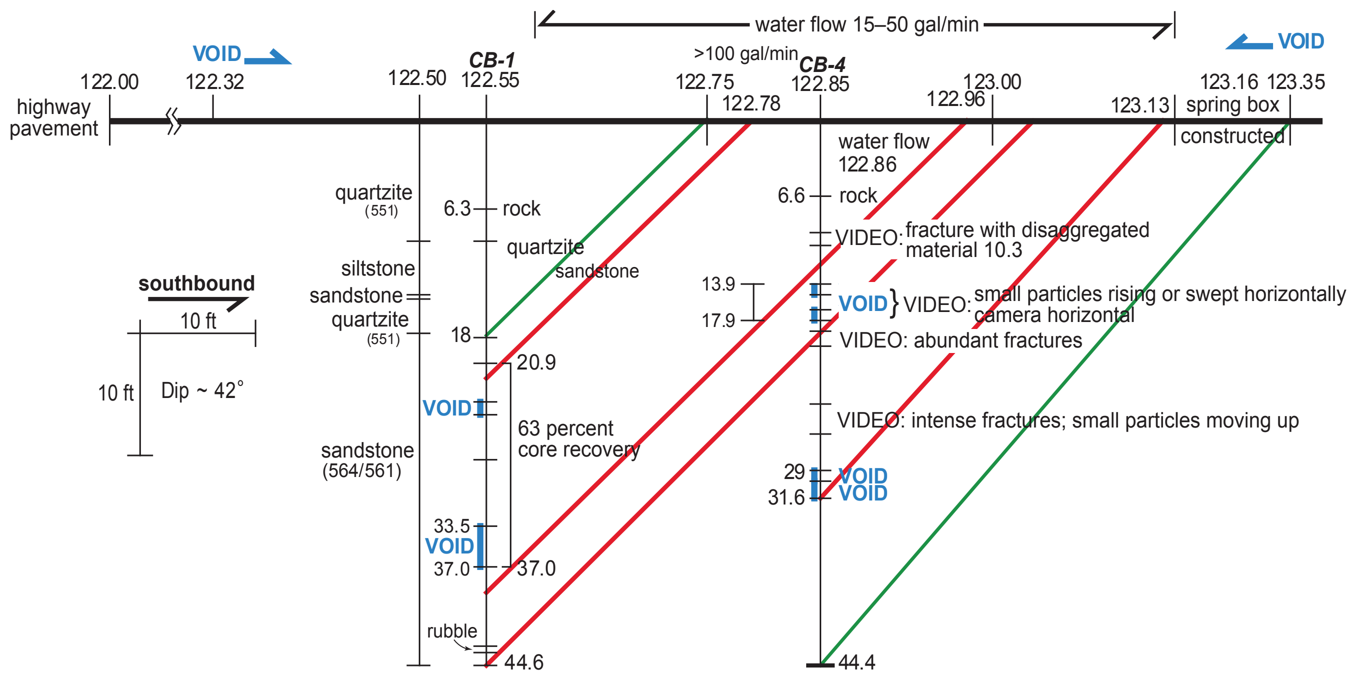

Figure 3. Longitudinal cross section of the southbound bore using data from CB-1 and CB-4.

outside walls between the southbound and northbound tubes. These variations produced offsets in the settlement void zones ranging from approximately 100 ft to 10 ft between the two tubes, which are apparent in ground penetrating radar mapping of void zones by the Kentucky Transportation Center. Strike and dip of the stratigraphic units have been generalized in the cross sections. The generalized dip is 42°, perpendicular to tunnel-tube alignment, although dip and strike of these strata as viewed in the full longitudinal profile of the tunnel tubes vary from the assumed approximations. This variation from the assumed approximations also contributed to the offset of void zones measured by ground penetrating radar in the two tunnel tubes.

Figure 3 is a longitudinal cross section of the southbound bore from stations 122.00 to 123.35. The aggregate void zone as defined by ground penetrating radar in August 2006 is between stations 122.32 and 123.35. Pertinent features mapped or recorded by Bhate Engineering were significant groundwater flow (15 to 50 gal/min) from the overlying bedrock from stations 122.58–123.13. Discharge was greater than 100 gal/min at station 122.75, so a spring box was constructed at station 123.16 to handle groundwater discharge at the tunnel invert.

CB-1 is located at station 122.55 and was cored to a depth of 44.6 ft (Fig. 3). There were several voids and core recovery was poor from 20.9–37.0 ft (63 percent recovery), indicating the presence of voids and fracture zones. Several voids that appeared in the video log corresponded with missing core. This zone of poor core recovery extends between stations 122.78 and 122.96 at the tunnel invert, which is approximately the center of the aggregate void zone beneath the highway pavement. Groundwater discharged at greater than 100 gal/min at station 122.75 (Fig. 3). This location is coincident with the top of the zone of poor core recovery at 20.9 ft in CB-1.

CB-4 is located at station 122.85, about in the center of the void mapped by ground penetrating radar (Fig. 3). The boring depth is 44.4 ft. The upper 20 ft of this core corresponds to the lower 20 ft of CB-1, an interval that includes the zone of poor core recovery. The video log of CB-4 provides evidence that the fracture and void zones seen in both core borings had active groundwater movement. In the fractured zones between 13.9 and 17.9 ft and 23.6 and 25.2 ft, small rock particles were being carried horizontally or upward in the borehole, and in the zone from 13.9–17.9 ft, the downhole cam-

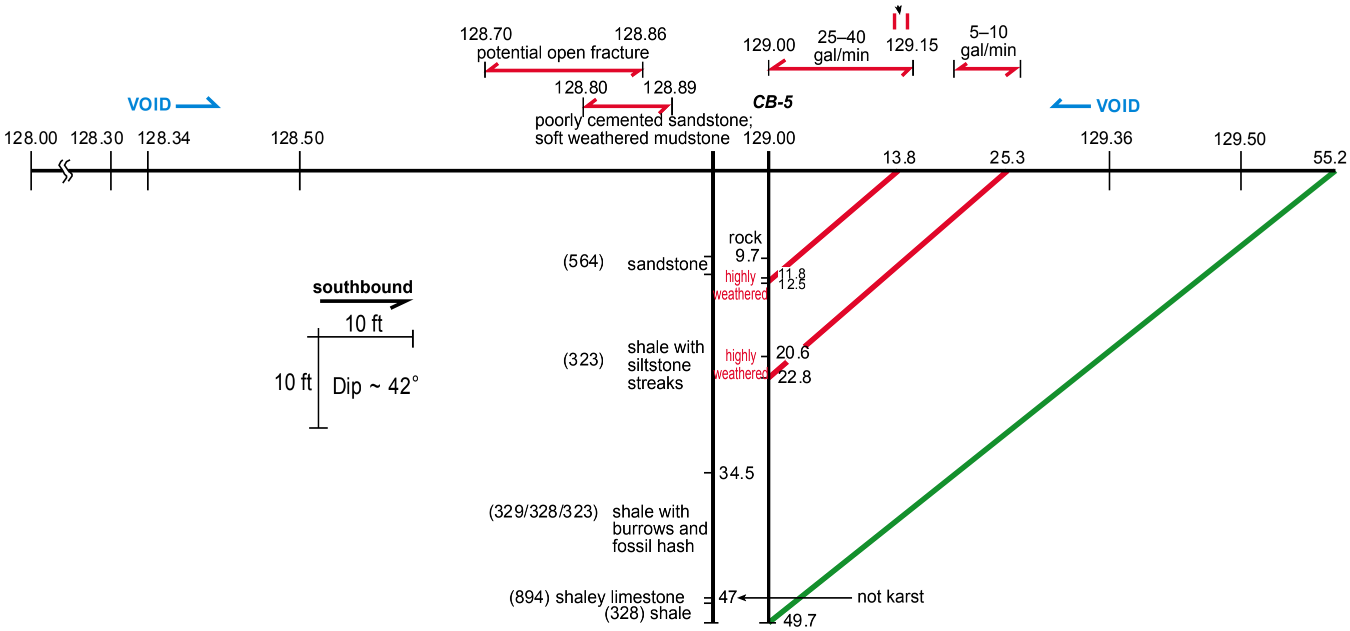

Figure 4. Longitudinal cross section of the southbound bore using data from CB-5.

era was moved sideways in the hole, indicating the strength and direction of groundwater movement in the borehole. Voids in the zone from 29.0 to 31.6 ft are equivalent to a tunnel invert location at station 123.13, very close to the spring box constructed at station 123.16, as noted by Bhate Engineering (1992).

Figure 4 is a longitudinal cross section of the southbound bore from stations 128.00 to 129.55. The aggregate void zone, as defined by ground penetrating radar in August 2006, was between stations 128.34 and 129.36. Only two highly weathered zones were logged in CB-5: one between 11.8 and 12.5 ft and the other between 20.6 and 22.8 ft. Groundwater discharge recorded by Bhate Engineering (1992) at the tunnel invert ranged from 5 to 40 gal/min and the water discharge zone included the two highly weathered zones as projected to the invert. Poorly cemented sandstone and soft, weathered mudstone was mapped by Bhate Engineering (1992) from approximately station 128.70 to 128.89, but this area is upsection from the core boring, so could not be used to confirm conditions below the tunnel invert (Fig. 4). CB-5 collapsed at about 11 ft depth shortly after drilling was completed, so the video camera could not be lowered into the hole. The invert during drilling was at a depth of 9.7 ft, probably 3 to 4 ft below the depth at which the tunnel invert is generally encountered. This could be the result of increased excavation of bedrock during the initial construction of the tube, or it could represent erosion of bedrock by groundwater flow since completion of the tunnel.

CB-2 and CB-3 were placed in the vicinity of the aggregate void measured by ground penetrating radar between stations 138.70 and 139.80 (Fig. 5). CB-2 is located at station 138.60, outside the aggregate void zone. Two weathered zones encountered at depths of 13.3–16.8 ft and 32.2–34.2 ft project updip into the aggregate void zone (Fig. 5). CB-3 encountered a void from 8.6–9.5 ft that may correspond to the lower weathered zone logged in CB-2 (32.2–34.2 ft). CB-3 also has two weathered fracture zones from 16.0–29.5 ft in depth and an intact sandstone layer that is 1.5 ft thick (Fig. 5). The upper fracture zone contains clay seams, indicating a high degree of weathering or potential transport of clay into a fracture zone by groundwater. The video log of CB-3 shows washout zones in the corehole where small rock particles were being swept horizontally and upward in the core boring by groundwater (Fig. 5). These zones project updip to the invert within the aggregate void zone between stations 139.07 and 139.22. Bhate Engineering (1992) did not report any major inflows of groundwater into the tube during construction within the aggregate void area, from stations 138.70 to 139.80.

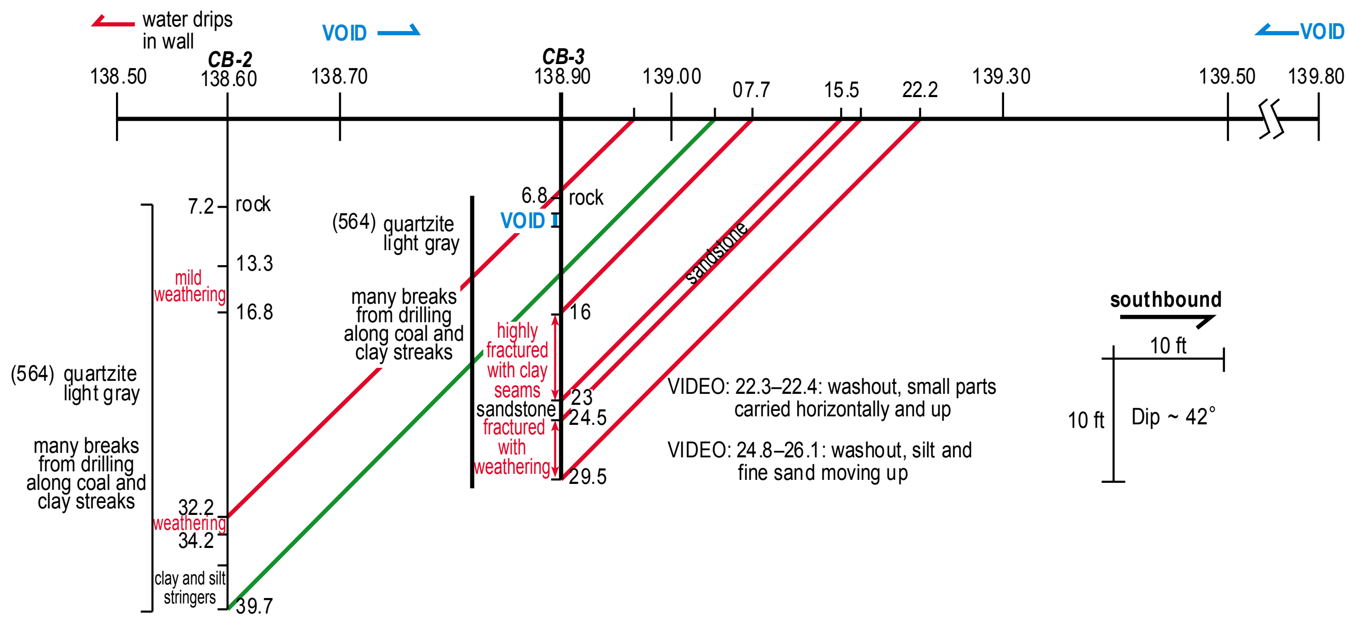

Figure 5. Longitudinal cross section of the southbound bore using data from CB-2 and CB-3.

Packer Tests. Packer tests were conducted in coreholes CB-3 and CB-4. There was limited time to conduct the tests, and we thought these two holes were most significant for confirming the direction and magnitude of the groundwater gradient in the bedrock beneath the roadway. Other coreholes of interest collapsed, and packer tests could not be conducted in some coreholes because the tunnel was being reopened. The zones in which heads were measured were determined by the presence of voids and fractures described in core logs and video logs.

Figure 6 displays the results from packer tests. In CB-3 and CB-4, groundwater hydraulic heads decreased upward. This demonstrates that groundwater flow in the bedrock beneath the tunnel is upward toward the tunnel invert and into the aggregate material. In CB-3, the upper monitored zone was centered around 16 ft depth and had a depth to water of 5.83 ft. This monitored zone is characterized by quartzite bedrock with fine coal streaks. This is likely competent rock with wider fracture separation and therefore a zone in which primary permeability plays a more active role than fracture permeability. In contrast, the lower zone, centered around 21 ft depth and a depth to water of 2.95 ft, occurs in a highly fractured quartzite. CB-4 shows a continual decrease in head up the borehole. The head loss was only 0.85 ft, compared to 2.88 ft measured in CB-3 from only half of that hole's depth. This difference may be the result of CB-4 exhibiting considerably more fractures than CB-3. Fracture flow would reduce the head necessary in CB-4 to direct groundwater in the bedrock from beneath the tunnel upward to the discharge zone at the tunnel invert.

Dye Tracing. A groundwater dye-tracing experiment was designed to determine if there were unknown losses of groundwater from the tunnel, using mass balance of the tracers. KGS also sought to determine if flow velocities were great enough to transport fine-grained particles, from either the crushed stone aggregate or from the bedrock (the hypothesis for the cause of the material being lost from the tunnel invert or roadbase). We also anticipated capturing some of the eroded rock materials and quantifying the rate of loss. The three types of tracers used were water-soluble fluorescent dye, insoluble and nearly neutral-buoyancy *Lycopodium* (club moss) spores, and insoluble and negative-buoyancy glass spheres. The flow velocity needed to move each of the three tracers differs substantially and therefore brackets the vector of the assumed upward flow velocity.

Two suites of tracers were injected through two locations in the southbound bore. The first injection location was at station 123.00, near CP-3, on May 3, 2006. Two-hundred fifty milliliters of 20 percent solution Rhodamine WT dye and 500 g

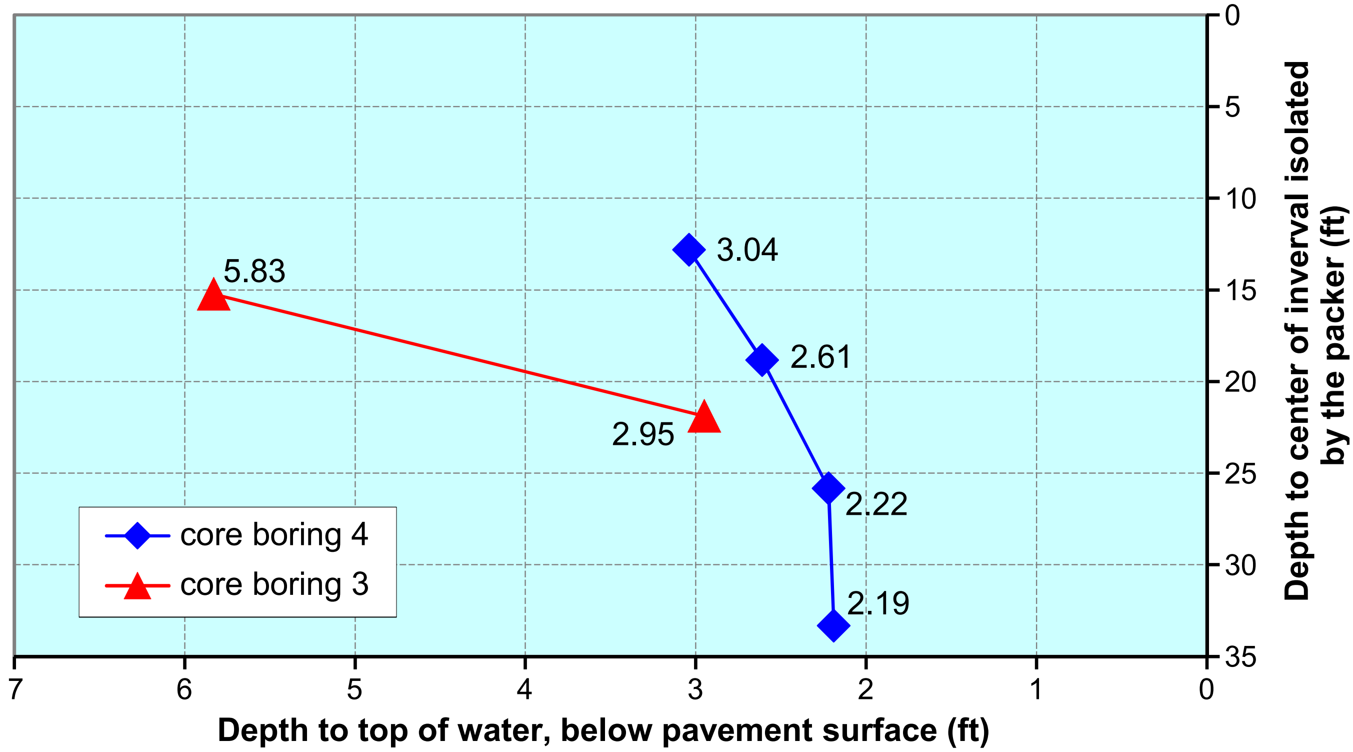

Figure 6. Groundwater head values for CB-3 and CB-4 as determined from straddle packer tests.

of *Lycopodium* spores were mixed with 5 gal of distilled water. Alconox surfactant was added incrementally to wet the spores until all were mixed with the solution. An estimated 1.4 million red glass spheres (diameter 0.5 mm, specific gravity 2.6 g/cm^3) totaling 688 g were washed in with the other two tracers. The injection process was very slow and lasted 1 hr, 13 min. The second injection site was located at station 128.75 near CP-5. The CP-5 injection used sodium fluorescein dye, premixed with water as described for the CP-3 trace, but no *Lycopodium* spores were used. An estimated 1.4 million green glass spheres (diameter 0.5 mm, specific gravity 2.6 g/cm^3), again totaling 688 g, were washed in with the dissolved tracer. Injection of the tracers on May 4, 2006, took 20 min.

Passive dye receptors were used to detect the arrival of dye at the junction boxes, the only point of access to the flow system. Trace receptors were packets of activated carbon charcoal attached to a concrete anchor or another tie point. Charcoal adsorbed the tracer as water and diluted dye flowed past the anchor point. Trace receptors were placed in the junction boxes at the guillotine gate weir, CP-1, CP-3, CP-4, CP-5, and CP-2½. CP-2½ was located in the roadway midline drain (Fig. 7).

The fluorescent dye mass discharged from the groundwater drainage system was determined from the dye concentration in water samples. The mass of the fluorescent dyes was measured before they were injected. The sampling for dyes was conducted with automatic sampling equipment. Concentration of dye in the water samples was determined with a fluorescence spectrophotometer. A dilution series was prepared to calibrate the instrument readings to concentration. Collection of samples to determine the background levels of fluorescent dyes or particulate tracers in the outflow from the tunnel at the guillotine gate began on April 28, 2006. At the time of tracer injection, both samplers were programmed to collect a sample every hour. Sampling was continued on an hourly schedule until dye from the CP-5 injection was observed in the bottles at the guillotine gate. Because the color in the bottles indicated the concentration was decreasing, the sampling frequency was then decreased to every 3 hr. Sampling stopped on May 18, 2006.

Date	CP-1 bug	CP-2.5 bug in under drain	CP-2.5 bug in collector	CP-3 bug		CP-4 bug		CP-5 bug
5/12			+ 6,807 –	+ 1,269 –		+ 1,028 –		– –
5/8			+ 5,370 –	+ 894 –				
5/5	+ 660 + 547	+ 21,332 –	+ 1,260 –	+ 1,386 –				
5/4	+ 506 + 579		+ 1,131 –					
5/3	– –	Placed May 5, 2006	– –	– –				
4/27	– –	Pulled June 14, 2006						

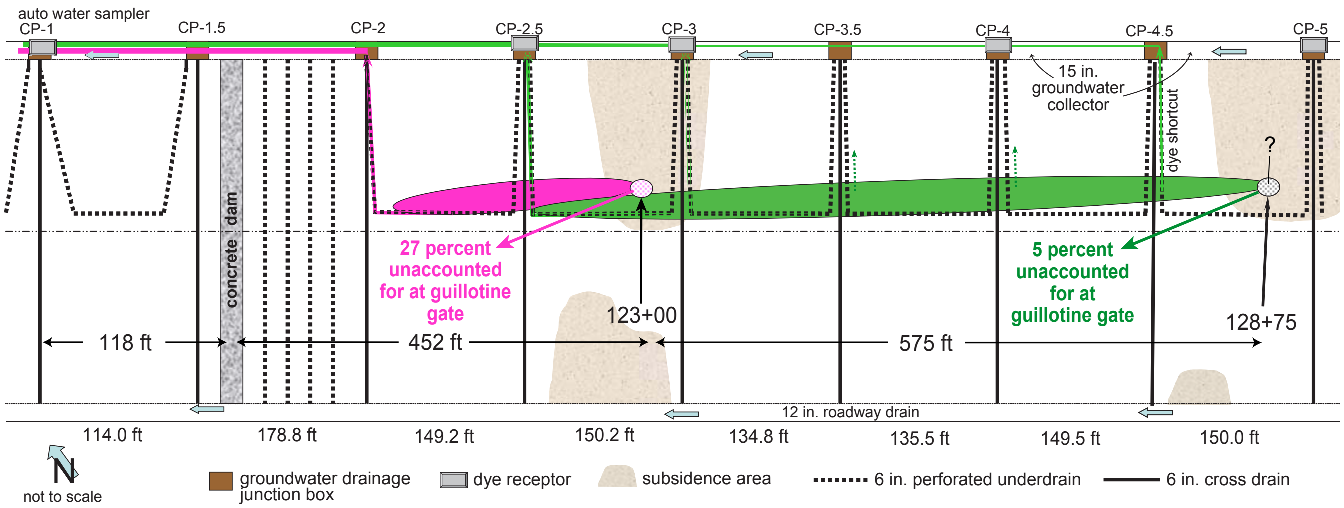

Figure 7. Schematic diagram of the southbound bore showing locations of dye detectors and the relative fluorescence response at each location.

The particulate tracers were monitored with commercially fabricated plankton nets with 100-ml and 250-ml sample bottles. The fabric retained particles with diameters greater than 25 µm, whereas the diameter of *Lycopodium* is nominally 35 µm. The bottles from the plankton nets were changed by Kentucky Geological Survey staff every visit through June 14, 2006. Later samples were collected weekly by the Cumberland Gap Tunnel Authority staff. Samples were examined for *Lycopodium* using palynological techniques and an optical research microscope. Suspended sediment was also collected by automated water sampler and by the same plankton nets used for the particulate tracers.

Flow velocity at the groundwater collector drains was measured at three junction boxes. These flow measurements were made with an electromagnetic flow meter, and the cross section was determined using the flow-in-pipes method (U.S. Department of Agriculture–Soil Conservation Service, 1956?). Velocity observations and calculated discharge values indicate a steady flow system, compared to a surface-flowing stream or a karst spring. Because the groundwater discharge rate was very steady, point measurements of flow were used to calculate mass flux, center of mass, and tracer recovery.

The tracer receptors allowed the route of the fluorescent dyes to be delineated with adequate detail. Figure 7 is a schematic diagram of the groundwater collection system and the subsidence areas in the southbound bore, and a summary of the trace receptor results. The presence or absence of a tracer for each monitored junction box is shown in the table at the top of Figure 7. The left (green) + or – symbols are for the fluorescein injected at CP-5 and the pink symbols are for the Rhodamine WT used at CP-3. All of the dye receptors were exposed to flow coming from the area upstream of the junction box, except at CP-2½, where an auxiliary dye receptor was used in the flow coming from the midline underdrain. It was only exposed to the groundwater underdrain flow and was positive for fluorescein.

The Rhodamine WT was not detected at the CP-2½ underdrain, but the receptor downstream at CP-1 was moderately positive for two consecutive receptors. No other tracer receptors inside the tunnel were positive for Rhodamine WT. The underdrain at CP-2 is the closest accessible monitoring point to an underground dam constructed between the CP-1½ junction box and CP-2. Although Figure 7 shows dye exiting the groundwater flow at CP-2, we speculate that a considerable percentage of the dye exited via the interior underdrains immediately upgradient of the underground dam.

The fluorescein injected at CP-5 followed a more complicated path than the Rhodamine WT did. A tracer receptor placed at CP-4 was positive despite being deployed on May 8. A receptor placed in the CP-5 junction box, a few feet upgradient of the injection site on the same date, was negative, as expected. The receptors at CP-3 and CP-2½ and all points downstream were clearly positive, including the receptor in the underdrain at CP-2½. The fluorescein plume may have been more dispersed by the time it reached CP-2½ than the Rhodamine WT was, as a result of distance traveled. Because the receptor at CP-4 also received flow from the junction box at CP-4½ and was positive and CP-5 was negative, the tracer began to flow into the groundwater collector at CP-4½, which resulted in a shortened travel time to the auto-samplers at CP-1 and the guillotine gate. The fluorescein flowing from the groundwater midline underdrain is probably the cause of the first peak in tracer seen in the water samples at CP-1 and the guillotine gate. The maximum peaks of the breakthrough curve are probably tracer that flowed through CP-2½ and CP-3, based on the relative intensity of the fluorescence in those receptors.

The quantitative traces resulted in a measure of the overall time of travel, and the mass recovery indicates that very little if any of the discharge is being lost from the system. The occurrence of peaks and the difference in their arrival times suggests a second way to calculate flow velocity in the subgrade material. Figures 8 and 9 illustrate the breakthrough curves of both tracers at CP-1 and the guillotine gate. The curves are in green and pink, representing the green fluorescein and dark pink Rhodamine WT, respectively. The graphs for the two sampling sites are very similar in regard to the overall shape of the curve and in the position of important peak concentrations.

Because of the presence of a complicated drainpipe system, accurately calculating ground-

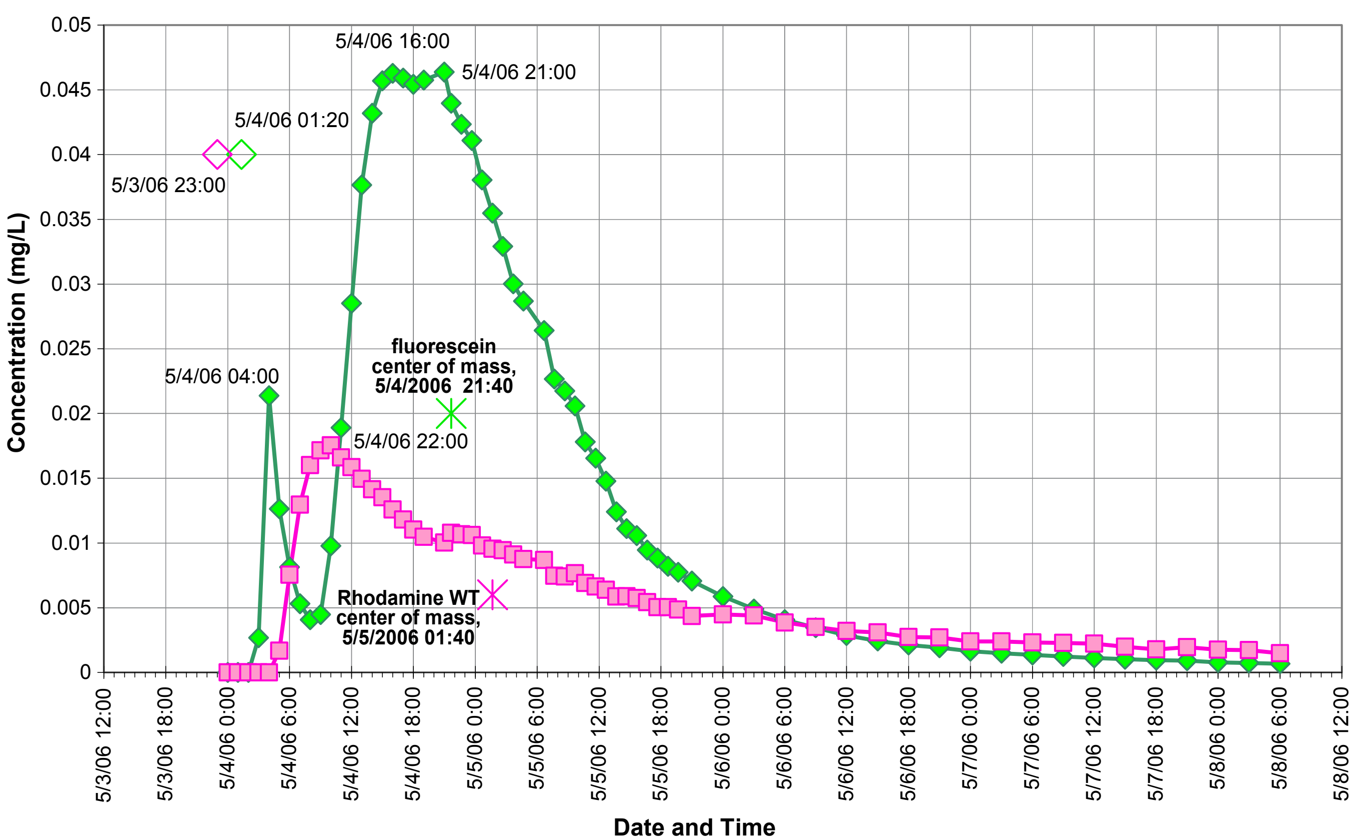

Figure 8. Dye concentration breakthrough curves for Rhodamine WT and sodium fluorescein at CP-1.

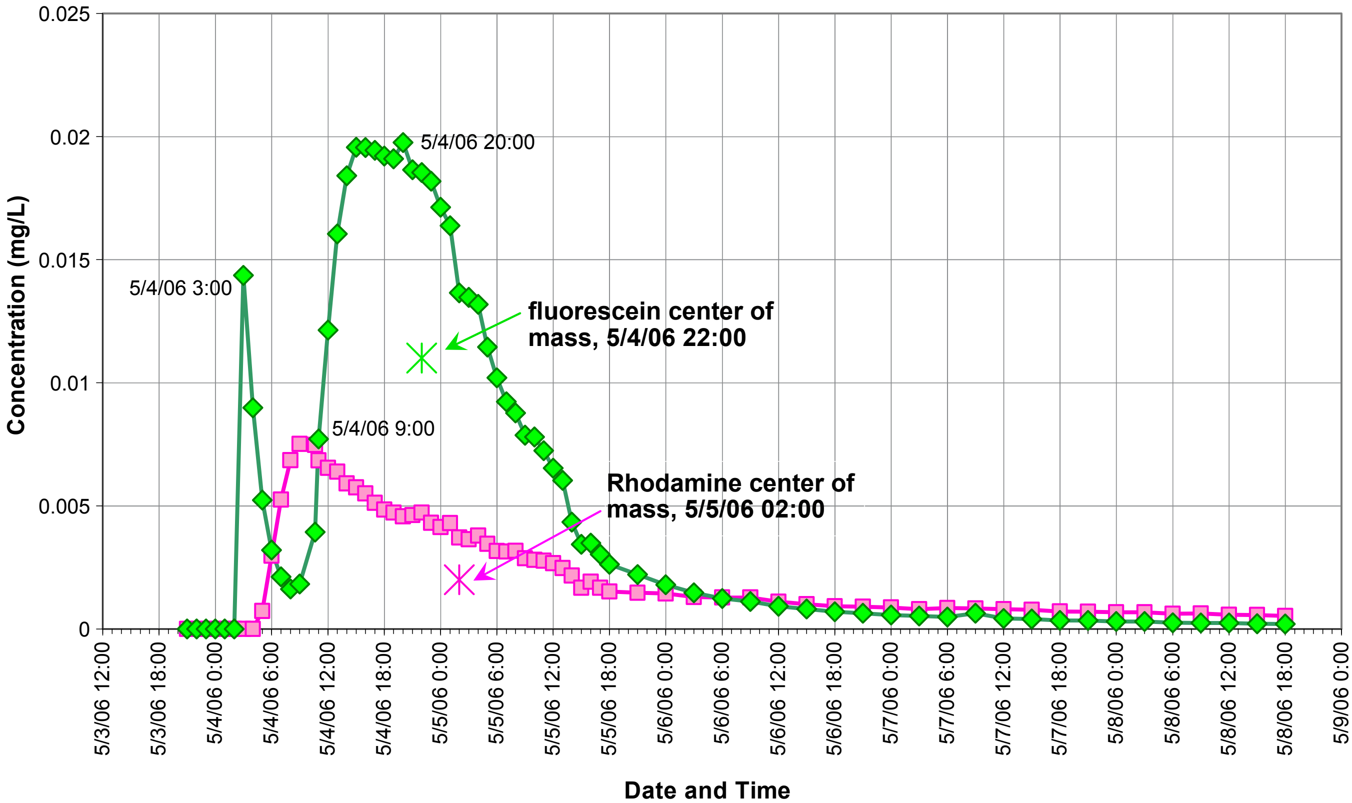

Figure 9. Dye concentration breakthrough curves for Rhodamine WT and sodium fluorescein at the guillotine gate.

water velocity using collected dye-tracing data is difficult, but the center-of-dye-mass data can be used to estimate possible range of the groundwater velocity. Assuming the dyes traveled between injection and recovery point in a straight line, the resulting velocities range from 0.006 to 0.028 ft/s (Table 2). In reality, the dyes traveled in the aggregate first and then entered the drainpipes; we could not determine the exact route because there were multiple underdrain pipes between the injection and receptor locations (Fig. 7). Using an average pipe flow velocity of 1.8 ft/s calculated from 10 measurements in the pipes between CP-5½ and CP-1 in July 2005, we estimated flow velocity in the aggregate for five possible flow routes (Table 3). These velocities ranged between 0.002 and 0.012 ft/s. All of the velocities presented in Table 3 were calculated assuming the flow route distance through the aggregate base was a straight line. Seepage velocity describes the actual velocity of the water following a tortuous path in the "manmade aquifer" medium. Using a porosity value of 0.32 for compacted aggregate (Burak, 2004), the estimated maximum seepage velocity was 0.038 ft/s.

All samples collected by plankton net were examined with a 60-power binocular microscope. Guillotine-gate samples and the CP-1 samples were further examined under a high-power optical microscope, as resuspensions of the filtrate, centrifuged concentrate of the resuspended filtrate, and residuum from leaching with aqua regia. No *Lycopodium* spores or glass spheres were found that could be identified as those injected by the Kentucky Geological Survey. *Lycopodium* and glass spheres that could be explained by local contamination were found, however. The background *Lycopodium* was at first thought to be the tracer, but further examination revealed that the back-

Table 2. Fluorescent dye-tracer flow velocities calculated using the straightline method.

Injection Location	*Receptor Location*	*Travel Time (s)*	*Velocity (ft/s)*
Near CP-5	CP-1	73,200	0.015
	guillotine gate	74,400	0.028
Near CP-3	CP-1	96,000	0.006
	guillotine gate	97,000	0.015

Table 3. Groundwater velocities in the aggregate estimated from aggregate-drain routes.

Dye Travel Route			*Distance in Pipe (ft)*	*Time in Pipe (s)*	*Distance in Aggregate (ft)*	*Time in Aggregate (s)*	*Velocity in Aggregate (ft/s)*
From	*To*	*Via*					
Near CP-5	CP-1	CP-4½	1,012.0	562.2	129.0	72,638	0.002
Near CP-5	CP-1	CP-2½	442.0	245.6	699.0	72,954	0.010
Near CP-5	CP-1	CP-2	292.8	162.7	848.0	73,037	0.012
Near CP-3	CP-1	CP-2	292.8	162.7	273.0	95,837	0.003
Near CP-3	CP-1	CP-1½	114.0	63.3	452.0	95,937	0.005

ground *Lycopodium* appeared only in the samples from the guillotine gate, which had contributions from surface runoff. Although isolation or filtration of the injected particulate tracers is highly probable, the flow velocity estimated using the dye tracing is too slow to move suspended load other than very fine silt and clay. Settling velocity of the spheres (0.12–0.22 ft/s) is an order of magnitude greater than the estimated maximum seepage velocity of 0.038 ft/s. Vertical settling velocity of *Lycopodium,* however, is three orders of magnitude less than for the spheres, at 0.0033 ft/s or about 28 ft/day (Harvey and Harms, 2002). *Lycopodium* could have been mobilized and should have arrived at the monitoring stations shortly after the dye arrived. One possible reason the *Lycopodium* spores were not detected is that they were trapped in the pores of the aggregate.

The sediment collected in the plankton nets was predominantly fine sand, typically well-rounded and frosted quartz; barely visible shards of glass, fragments of fresh vitreous coal, flakes of rusted steel, sawdust, and countless fragments of insects and bits of vegetation were also collected. The sediment sample had a similar composition and size distribution as a debris sample collected from the joint between the lid of the junction box and the other material that had accumulated on the saddle-T, a plastic pipe fitting that holds the plankton net onto the midline drain.

Summary of the First Phase Activities. The core drilling showed multiple zones of voids, fractures, and weathered rocks, but no particular lithologic unit seems to be more common in settlement zones than any other lithologic unit. There is groundwater inflow at all locations where void zones have been mapped. Packer tests in CB-3 and CB-4 verified that groundwater flow is upward in the bedrock from beneath the tunnel, toward the invert of the tunnel where it discharges into the aggregate. Inflow of groundwater ranged from approximately 5 to more than 100 gal/min in the two void zones in which core drilling took place.

Dye tracing indicated that all the groundwater entering the tunnel aggregate was being transported through the designed drainage system; there was no extraneous groundwater flow out of the tunnel that could carry rock material from the tunnel unobserved. Dye tracing also indicated that groundwater velocity in the aggregate was too slow to suspend and transport the 0.5-mm glass spheres, but could move *Lycopodium. Lycopodium* was not detected, however, and the most likely explanation is that the *Lycopodium* spores were trapped in the pores of the aggregate.

Second Phase: Groundwater Chemistry Investigations

In June 2007, a 115-ft-long section of the highway pavement and underlying limestone aggregate were excavated from a subsidence zone in the southbound bore, in the vicinity of CP-3, between stations 122.25 and 123.40. After the aggregate was excavated, several high-volume springs were observed on the bedrock floor, one having a pH of 6.0. The bedrock invert was found to be firm, and no soft spots or voids were observed into which the aggregate could move and accumulate. Individual pieces of the limestone aggregate showed dissolution surface features similar to those observed in karst terrains. These features include rounded edges of formerly sharp breakage surfaces, pitting of surfaces, and raised relief of resistant chert inclusions on aggregate surfaces (Fig. 10). In addition, aggregate-size analysis by the Kentucky Transportation Center indicated that the limestone aggregate removed from the excavation was deficient in small particles, and that large particles

Figure 10. Sample of limestone aggregate recovered during June 2007.

were reduced in size by approximately 30 percent compared to standards for No. 57 aggregate. During the excavation of the aggregate, several void arches were noted in close proximity to the invert; the voids were approximately 6 in. high and 18 in. wide. The cement surface of the mud wall was etched, exposing coarse-grained clastic in the concrete wall. These features and measurements indicate that the limestone aggregate material is being dissolved by water moving through it. This strongly suggests that limestone aggregate dissolution by groundwater is a principal cause for the voids in the aggregate and subsequent subsidence of the roadway pavement. A more detailed description of aggregate removal can be found in Rister (2010).

To determine what processes control the dissolution of the limestone by groundwater, KGS collected precipitation, groundwater-discharge, and groundwater-quality data from July 2007 to September 2009. Other objectives were to estimate the mass flux of material being dissolved from the limestone aggregate by the groundwater and to understand the response of the water quality when the void in the vicinity of CP-3 was filled with granite aggregate.

Groundwater Discharge Monitoring. Once we suspected that the dissolution mechanism was the primary source of pavement deflection, a more accurate method of flow needed to be established for each of the bores in order to determine the dissolved mass flux of limestone exiting the bores. In October 2007, KGS installed a stage recorder and developed a rating curve for the combined discharge at the collection box of the guillotine-gate drop culvert, approximately 750 ft downstream (northwest) of the tunnel entrance. A 90° V-notch weir and stage-recording device were installed in the clean-out box at CP-1 in both the northbound and southbound tunnels on February 20, 2008. Some surface water was drained to the guillotine gage during precipitation, and the stage-discharge rating curve developed is not considered to be accurate because of the small size of the collection box at the drop culvert, which causes turbulent flow.

Figure 11 illustrates groundwater-discharge behavior recorded at the northbound and southbound bores from February 2008 to June 2008, as well as precipitation events. The northbound bore flow exhibits a pronounced flashy flow with respect to precipitation events, compared to flow in the southbound bore. The groundwater flow in both bores is to the north. The relatively flashy behavior of the northbound flow associated with precipitation events strongly suggests that the northbound bore is being influenced by discharge from the cave system in the vicinity of station 147.00. The exact locations of any connections between the cave system located by Golder Associates in 1987 and the northbound bore are undetermined. Water in the cave system was routed beneath the bores via an inverted siphon installed during tunnel construction. Field inspection revealed no obvious means of cave water entering the bores, and construction records indicate no direct connection of the cave system to either bore. During the five separate water-quality sampling events, the two most upgradient wells in the southbound bore contained insignificant amounts of groundwater, whereas wells in the northbound bore contained sufficient water to be sampled. This is another indication that the northbound bore is receiving recharge from the

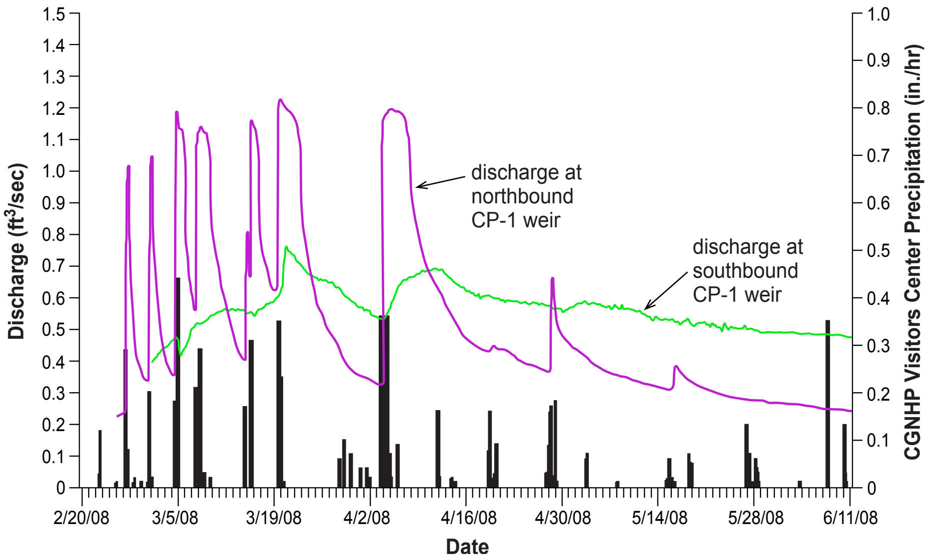

Figure 11. Discharges from the southbound and northbound bores.

cave system but the southbound bore is not, or at a minimum compared to the northbound bore.

Water-Chemistry Investigations

Groundwater Monitoring Wells in Tunnel Bores. Wells were installed in both bores of the tunnel to monitor groundwater depth and chemistry, primarily in the limestone aggregate, and in groundwater discharging from the bedrock that is recharging the aggregate. Twenty-seven wells were installed in the southbound bore in August 2007, and 23 were installed in the northbound bore in September 2007. The primary objective of these wells was to determine changes in groundwater chemistry upgradient, within, and downgradient of each of the void zones. Two wells in each bore were installed in sectors of the bores characterized by limestone bedrock to obtain background information. An additional 34 wells were installed in 2009: 15 in the southbound bore and 19 in the northbound bore. The goal for the additional wells was to help us understand the water chemistry where voids have not developed.

Cores were drilled through the concrete pavement, and the wells were pushed through augured gravel aggregate or through a drive pipe to refusal, which was assumed to be the tunnel invert. Most of the wells are approximately 5 ft in length, are constructed of 0.75-in.-diameter schedule-40 PVC, are finished below the upper pavement surface, and have a surface cap. Most wells extended through the approximately 4 ft of limestone aggregate to the bedrock invert, and have a 0.9-ft-long screen at their base for monitoring water. One well (SB2) was completed through the granite aggregate to monitor a spring boil observed at the invert during excavation and replacement of the limestone aggregate in June 2007.

Wells were pumped with a peristaltic pump when they were installed and for several weeks after installation to remove clay and fine silt that accumulated in them during installation. In several instances, wells were reinstalled with a section of blank casing beneath their screens when the sediment could not be cleaned out of the original well.

The monitoring wells were sampled five times. Two of the sampling events occurred during low-flow conditions and the other three samples were taken during higher-flow conditions. The low-flow samples were collected on October 9–10, 2007, and November 5–6, 2007. The higher-flow samples were collected on April 7–8, 2008, May 27–28, 2009, and August 26–27, 2009. The 50 wells installed in 2007 were all sampled during the first three sampling events; 19 of them were sampled again in 2009, of which 17 were sampled during the last two sampling events and the other two during the last sampling event. The additional wells installed in 2009 were all sampled during the last two sampling events. Groundwater samples were also collected in seven cross passages during the first two sampling events. Southbound cross passage 3 (SBCP-3new) was sampled a third time during the last sampling event. Cave water was sampled in both bores in August 2008.

Calcite Saturation Index Calculation and Interpretation. The groundwater samples in the tunnels were collected to characterize the chemistry of the groundwater as it moved through the aggregate. The calcite saturation index was calculated to determine what controls dissolution of calcite, the primary mineral in the limestone roadbase aggregate.

The calcite saturation index was calculated using PHREEQC geochemical software (Parkhurst and Appelo, 1999). In general, a negative saturation index indicates that the water will dissolve calcite (termed “aggressive with respect to calcite/limestone”), and a zero or positive saturation index indicates that the water will not dissolve calcite (i.e., it is saturated with respect to calcite). The higher the absolute value of the saturation index, the greater a water sample’s ability to react in the fashion designated by the negative or positive sign. For example, water with a saturation index of –1.4 is more aggressive than water with a saturation index of –0.2.

Sensitivity analysis of the water-quality variables pH, temperature, and calcium, and bicarbonate concentrations for the water-quality data sets collected for this study indicate that pH is the most significant variable and that samples having a saturation index of 0.1 to –0.10 are near neutral, whereas those having a saturation index less than –0.10 are aggressive with respect to calcite.

The saturation indices show that most of the groundwater in this part of both tunnel bores is aggressive with respect to calcite (i.e., the groundwater will dissolve this mineral over time) (Tables 4–5). As for the worst-case saturation index (the minimum) for each well, all wells except one (SB4C) in the southbound bore are aggressive with respect to calcite. In the northbound bore, all wells except two (NB06 and NB16A) are aggressive with respect to calcite. Out of all water-quality samples analyzed from wells through five rounds of sampling, 84 percent of the southbound samples were aggressive with respect to calcite and 77 percent of the northbound samples were aggressive with respect to calcite.

Data from the wells installed near the void zone suggest that most of the nonaggressive water was collected during low flow (six sites out of 27 sites). This is expected, as the lower the flow, the smaller the velocity of groundwater movement. Slower velocity allows the groundwater to react with the calcite more readily than with faster velocity, and allows the water to approach or come into chemical equilibrium with respect to calcite. Subsequently, dissolution of calcite is either slowed or halted.

Groundwater was also measured in the groundwater collection pipe along the inner mud wall at seven locations and once in the cave between stations 146.00 and 151.00 discovered by Golder Associates in 1987 (Table 6). Location SBCP-3new had very aggressive water, as expected (saturation index was –2.68 in August 2009). The groundwater monitored in this location included water collected beneath the roadway pavement from stations 122.25 to 123.40, where the limestone aggregate was replaced by granite aggregate in 2007. As anticipated, the minerals in the granite are apparently not being dissolved by the aggressive bedrock groundwater. Without the dissolution chemical reaction, the groundwater recharge remains aggressive as it comes out from the bedrock invert. At other collection-pipe locations except SBCP-7.5, the groundwater is aggressive with respect to calcite, but to a lesser extent, similar to groundwater outflow downgradient from the void zones. The cave water collected in 2008 showed positive calcite saturation values, indicating that water leaked into the collection system from the cave is not aggressive with respect to calcite.

Third Phase: Limestone Aggregate Dissolution Experiment

Water-chemistry analysis confirmed that groundwater in the aggregate is capable of dissolving the limestone aggregate; however, how fast the aggregate is being dissolved was not well quantified. To determine the rate of dissolution, the Kentucky Geological Survey installed retrievable limestone aggregate baskets in different locations beneath the roadbed and measured the mass loss of the baskets through time. The baskets were installed in the tunnels in October 2011. The initial plan was to measure the mass loss twice a year for several years until the road was repaired. But the section of road where the baskets were installed was repaired between January and May 2012, much earlier than expected. Therefore, all the baskets were taken out in March 2012. As a result, the baskets were only weighed twice, during their installation and removal.

Table 4. Calculated calcite saturation indices from the southbound bore from 2007 to 2009. Blank cells = data not collected.

Site ID	*Station Number*	*Calcite Saturation Index of Southbound Bore*					*Minimum Value*
		Oct. 2007	*Nov. 2007*	*April 2008*	*June 2009*	*Aug. 2009*	
SB1A	115.01				dry	dry	dry
SB1B	119.50				–0.05	–0.34	–0.34
SB1C	120.67				–0.07	–0.35	–0.35
SB1D	121.95				–0.41	–1.15	–1.15
SB01	122.15	–0.22	–0.55	–0.64	–0.74	–2.07	–2.07
SB02	123.11	–0.39	–0.35	–1.07			–1.07
SB03	123.50	–0.38	–0.32	–0.41	–0.02	–0.79	–0.79
SB4A	123.75				–0.10	–0.41	–0.41
SB4B	124.40				0.60	–0.13	–0.13
SB4C	125.55				–0.07	–0.07	–0.07
SB04	125.80	–0.18	–0.18	–0.61	–0.22	–0.36	–0.61
SB05	125.95	–0.52	–0.26	–1.25			–1.25
SB06	126.08	–0.22	–0.01	–0.35	–0.06	–0.35	–0.35
SB7A	126.84				–0.05	–0.15	–0.15
SB07	127.40	–0.51	–0.26	–0.58	–0.59	–0.38	–0.59
SB08	127.56	0.10	0.05	–0.70		–0.54	–0.70
SB09	127.72	–0.38	–0.01	–0.40		–0.24	–0.40
SB10	128.17	–0.11	–0.13	–0.30			–0.30
SB11	128.26	–0.68	–0.07	–0.65			–0.68
SB12	128.27	–0.18	–0.07	–0.10			–0.18
SB13	128.50	–0.24	–0.16	–0.20			–0.24
SB14	128.73	–1.02	–0.94	–1.63	–1.70	–1.39	–1.70
SB15	129.00	–1.36	–1.61	–1.71			–1.71
SB16	129.20	–0.30	–0.01	–0.16	–0.27	–0.05	–0.30
SB17A	129.70				–0.17	–0.03	–0.17
SB17B	132.00				–0.62	–0.55	–0.62
SB17C	133.86				–0.54	–0.60	–0.60
SB17D	134.99				–0.70	–0.14	–0.70
SB17E	136.00				–0.73	–0.15	–0.73
SB17F	137.62				–0.65	–0.15	–0.65
SB17	137.87	–0.28	–0.51	–0.54	–0.89	–0.46	–0.89
SB18	138.05	–0.90	–0.78	–1.02			–1.02
SB19	138.23	–0.19	–0.28	–0.31			–0.31
SB20	138.60	–0.17	–0.21	–0.35			–0.35
SB21	138.90	–4.28	–3.71	–4.42			–4.42
SB22	139.01	–2.43	–2.23	–2.12			–2.43
SB23	139.36	–0.37	–0.11	–0.38			–0.38
SB24	139.70	–2.37	–2.92	–0.66			–2.92
SB25	139.89	0.04	–0.59	–0.18	–0.43	0.05	–0.59
SB26A	140.14				–0.45	–0.04	–0.45
SB26	142.40	dry	dry	dry	dry	dry	dry
SB27	149.90	dry	dry	dry	dry	dry	dry

Table 5. Calculated calcite saturation indices from the northbound bore from 2007 to 2009. Blank cells = data not collected.

Site ID	*Station Number*	*Calcite Saturation Index of Northbound Bore*					*Minimum Value*
		Oct. 2007	*Nov. 2007*	*April 2008*	*June 2009*	*Aug. 2009*	
NB1A	115.01				dry	dry	dry
NB1B	119.50				–0.07	–0.24	–0.24
NB1C	120.25				–0.62	–0.83	–0.83
NB01	120.50	–0.53	–0.30	–0.29	–0.44	–0.34	–0.53
NB02	120.67	–1.12	–0.79	–0.94			–1.12
NB03	120.85	–0.47	–0.01	–0.32	–0.72	–0.76	–0.76
NB4A	121.10				–0.10	–0.29	–0.29
NB4B	122.02				–0.05	–0.29	–0.29
NB04	122.27	–0.11	–0.10	–0.07	–0.14	–0.30	–0.30
NB05	122.52	–0.47	–0.06	–0.39			–0.47
NB06	122.81	–0.01	0.00	0.03			–0.01
NB07	123.08	–0.05	–0.25	–0.01			–0.25
NB08	123.30	–0.08	–0.23	–0.31	–0.04	–0.30	–0.31
NB9A	123.55				–0.26	–0.23	–0.26
NB9B	124.40				–0.17	–0.24	–0.24
NB9C	125.95				–0.05	–0.29	–0.29
NB9D	126.60				–0.18	–0.12	–0.18
NB09	126.84	–0.35	–0.34	–0.40	–0.18	–0.14	–0.40
NB10	127.14	–0.52	–0.58	–1.15			–1.15
NB11	127.35	–0.58	–0.11	–0.73			–0.73
NB12	127.74	–0.44	–0.33	–0.13			–0.44
NB13	128.56	–0.53	–0.29	–0.32			–0.53
NB14	128.73	–0.77	–0.40	–0.66			–0.77
NB15	128.92	–0.49	–0.38	–0.30	–0.27	–0.20	–0.49
NB16A	129.21				–0.06	–0.05	–0.06
NB16B	129.70				–0.72	–0.06	–0.72
NB16C	132.00				–1.10	–0.20	–1.10
NB16D	133.86				–1.17	–0.27	–1.17
NB16E	134.48				–0.76	–0.24	–0.76
NB16	134.84	–0.53	–0.14	–0.10	–0.36	–0.25	–0.53
NB17	134.99	–0.09	–0.13	0.02			–0.13
NB18	135.18	–0.16	–0.33	–0.08			–0.33
NB19A	135.33				–0.87	–0.69	–0.87
NB19B	136.00				–0.58	–0.31	–0.58
NB19C	136.25				–0.55	–0.05	–0.55
NB19D	138.48				–0.67	–0.17	–0.67
NB19	138.73	–0.58	–0.32	–0.66	–0.72	–0.11	–0.72
NB20	139.15	–0.42	–0.12	–0.80			–0.80
NB21	139.48	–0.61	–0.37	0.19	–0.23	0.05	–0.61
NB22A	139.73				–0.50	0.05	–0.50
NB22	142.50	–0.32	–0.09	0.22	–0.12	0.04	–0.32
NB23	150.00	–0.19	–0.08	0.40	0.23	0.27	–0.19

Table 6. Calculated calcite saturation indices from the cross passages and the cave. Blank cell = data not collected.

Site ID	Station Number	Calcite Saturation Index			
		Oct. 2007	Nov. 2007	Aug. 2008	Aug. 2009
NBCP01	115.01	–0.64	–0.39		
NBCP03	122.35	–0.91	–0.50		
NBCP4½	127.45	–1.20	–0.63		
NBCP7½	136.10	dry	dry		
SBCP-1	115.01	–0.75	–0.78		
SBCP-3new	122.35	–1.83	–1.50		–2.68
SBCP-4½	127.45	–0.45	–0.28		
SBCP-7½	136.10	0.35	0.11		
Cave-SB	145.40			0.20	
Cave-NB	145.40			0.22	

Aggregate Basket Installation and Data Collection. Two sites in the northbound tunnel were selected for the dissolution experiment. Ground penetrating radar data from the first site at station 131.50 showed no noticeable voids, but water was relatively more aggressive with respect to calcite, as indicated by the previous water-chemistry investigation. The other site at station 139.30 was in a void zone identified by ground penetrating radar. Two boreholes, one in each lane, were drilled through the roadbed aggregate at each site. The boreholes were of 2-in. diameter and cased with PVC pipe on top and PVC screen of 3/8 in. to the bottom. The four boreholes were drilled in November 2010. Four water samples, one for each borehole, were taken on August 17, 2011. One additional water sample was collected at CP-1. Water level, temperature, pH, and electrical conductivity were measured at the five sites. A stage recorder was installed at CP-1 to collect water-level data every 10 min during the experiment. The water-level data were used to estimate discharge using a rating curve.

Ten stainless-steel mesh baskets (1.5 in. diameter and 15 in. length) were filled with limestone aggregate recovered from the borehole drilling. Eight of the baskets were installed in the boreholes, with two baskets vertically stacked in each borehole. The other two baskets were kept in a laboratory at the Kentucky Transportation Center as controls. Prior to being deployed in the tunnel, the baskets were weighed (oven-dry) using a digital scale with a precision of 0.1 g. The same scale was used throughout the experiment. Initial masses of the baskets ranged from 597 to 609 g (Table 7). These baskets were installed in the northbound tunnel on October 4, 2011. The percentage of each basket submerged in water was estimated in the field (Table 7). No water samples were taken during the basket installation because the flow condition was similar to the flow on August 17, 2011, when water samples were initially taken. The baskets were pulled from the boreholes on March 20,

Table 7. Basket masses and submergence percentages.

Site Location	Basket Location	Submerged in Water (%)		Mass (g)		Mass Loss (g)
		10/4/2011	3/20/2012	10/4/2011	3/30/2012	
Station 131.50 right lane	top	40	45	597.5	597.0	0.5
	bottom	100	100	608.8	608.2	0.6
Station 131.50 left lane	top	75	90	600.0	597.1	2.9
	bottom	100	100	599.7	596.6	3.1
Station 139.30 right lane	top	30	60	597.1	596.7	0.4
	bottom	100	100	597.8	596.7	1.1
Station 139.30 left lane	top	0	0	599.4	599.1	0.3
	bottom	80	100	598.0	584.1	13.9
Reference basket 1	N/A	N/A	N/A	602.4	602.5	–0.1
Reference basket 2	N/A	N/A	N/A	599.6	599.7	–0.1

2012. Water samples, field water levels, and field water-chemistry measurements were taken on the same day. The baskets were brought to a laboratory at the Kentucky Transportation Center and weighed (oven-dry) on March 30, 2012.

Basket Mass and Water-Chemistry Analysis. The aggregate mass data show that all the baskets installed in the aggregate lost mass during the experimental period of 178 days (Table 7). The largest mass loss occurred in the bottom basket installed in the left lane of station 139.30. The basket lost 13.9 g or 3.4 percent of rock (this basket had initial mass of 410.6 g). If this mass loss rate continued, all the limestone aggregate in the basket would be dissolved away in less than 15 yr. The smallest mass loss also occurred at the same site, but in the top basket. This basket was entirely above water on both sampling days and only lost 0.3 g. We think the small loss was caused by some high-flow events that inundated part of the basket for some short periods. The contrast in mass loss between the two baskets directly supports our hypothesis that dissolution of calcite by groundwater is the cause for the loss of limestone aggregate. All other top baskets also had a smaller volume submerged in water and smaller mass loss than their bottom counterparts, which again demonstrates that dissolution by aggressive water is the cause for the mass loss. The two reference baskets (Table 7) showed little mass change, showing that the balance used for measuring mass was precise.

Calcite saturation indices (Table 8) show that water from all four sites is aggressive with respect to calcite, except for the sample taken from the right lane of station 131.50 on August 17, 2011. For all five sites, the water samples taken on August 17, 2011, were less aggressive with respect to calcite than the samples taken on March 20, 2012. The basket submergence data (Table 7) showed that water levels on the later date were higher than on the first date, indicating that water flow velocity was higher on the later date. Higher water velocity leaves less time for water from upstream or bedrock to react with limestone; therefore, water is less buffered and remains aggressive with respect to calcite. The saturation indices also show that water chemistry is not spatially homogeneous, even between two lanes at the same time; this is also evident from water-chemistry analysis. For example, when pulled from the borehole, the bottom basket from the left lane at station 131.50 was covered with a red iron stain (Fig. 12), whereas the bottom basket from the right lane showed no iron stain. The water samples taken from the left lane had iron concentrations of 1.11 and 2.18 mg/L for the two sampling dates. Iron concentration of the water samples from the right lane were less than the detection limit of 0.002 mg/L for the same two sampling dates, however.

The varying water chemistry appears to play a major role in controlling the rate of limestone aggregate mass loss. Figure 13 is a scatter plot of calcite saturation indices on March 20, 2012, versus bottom basket mass loss, showing that the rate of mass loss is strongly associated with the aggressiveness of the groundwater. The figure indicates that more aggressive water is capable of dissolving limestone more quickly. The figure also partially explains that the mass losses among boreholes are significantly different, even between the left and right lanes at the same station.

Table 8. Calcite saturation indices for water samples during the dissolution experiment.

Site Location	*Calcite Saturation Index*	
	8/17/2011	*3/20/2012*
CP-1	–0.25	–0.78
station 131.50, left lane	–0.34	–0.69
station 131.50, right lane	–0.02	–0.19
station 139.30, left lane	–0.68	–1.38
station 139.30, right lane	–0.07	–0.37

Summary and Conclusions

This hydrologic investigation of the road subsidence in the Cumberland Gap Tunnel has lasted almost 7 yr. A variety of methods were used to investigate the causes of the subsidence. The initial focus was on bedrock and groundwater flow characterization to see if bedrock weathering was causing the road to settle. After realizing that a huge volume of groundwater was flowing in the roadbed aggregate, we geared our efforts to testing if the water flow is fast enough to carry small particles from the aggregate. Groundwater tracing suggested, however, that the flow is not fast enough to physically erode the aggregate. An excavation of a short section of roadbed in 2007 offered a unique opportunity to observe aggregate, groundwater,

Figure 12. The bottom basket in the left lane of station 131.50 in the northbound tunnel on March 20, 2012, had iron staining.

and the road drainage system. These observations led us to suspect that the dissolution of limestone aggregate by groundwater is a possible major process responsible for the road subsidence. We then focused on collecting and analyzing water chemistry data. Calcite saturation indices calculated from 265 water samples collected along the tunnels from 2007 to 2009 showed that the water in the roadbed aggregate is capable of dissolving calcite, the major mineral of the limestone aggregate. To further understand the rate of dissolution, an experiment was conducted in the field from 2010 to 2012. The hydrogeologic investigations helped the Kentucky Transportation Cabinet, Tennessee Department of Transportation, U.S. National Park Service, Kentucky Transportation Center, and Kentucky Geological Survey to design a long-term repair for the problem. The subsidence stems from the use of limestone as aggregate base.

In summary:

1. Dissolution of calcite by groundwater causes the limestone aggregate to lose mass. The mass loss leads to voids forming beneath the roadbed and eventually to roadway subsidence.
2. The rate of aggregate mass loss varies in different areas in the tunnel. The variation is controlled by flow rate and chemistry of water discharging from the surrounding bedrock. Water that is more aggressive with respect to calcite is capable of removing limestone aggregate more quickly. Water during high-flow conditions appears to be more aggressive with respect to calcite and removes the aggregate faster than water during low-flow conditions.
3. Groundwater velocity in the bedrock fractures and voids is sufficient to move sand and smaller particles upward and horizontally in some locations. But dye tracing indicated that groundwater velocity in the aggregate was too slow to be a major force in removing a significant amount of mass from the roadbed.
4. Dye recovery indicated that all the groundwater entering the tunnel aggregate is being transported through the designed drainage system; there is no extraneous groundwater flow out of the tunnel that could carry rock material from the tunnel unobserved.

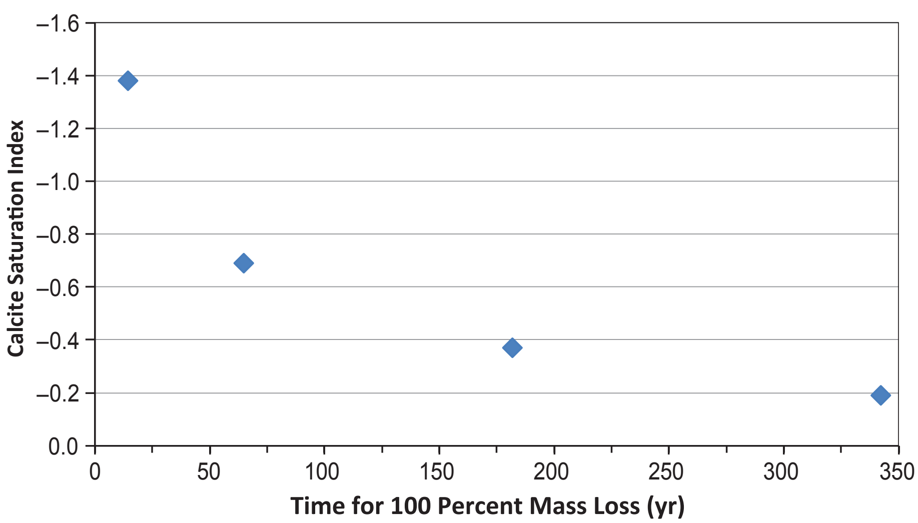

Figure 13. Scatter plot of bottom basket mass losses versus calcite saturation indices.

Acknowledgments

This investigation was funded by grant KTC-10-03/KH58-07-1F and partially funded by Tunnel Management Inc. This study involved extensive field work, for which we thank Glynn Beck, Bart Davidson, Mike Farwell, Randy Paylor, and Scott Waninger from the Kentucky Geological Survey at the University of Kentucky; Tim Jones, Tim Scully, Jamie Creech, Levi McIntosh, and Eddie Jordan from the Kentucky Transportation Center at the University of Kentucky; Chuck Knowles, Sherri Greenwell, Rusty Wallace, Mike Calebs, Paul Looney, and Nancy Albright from the Kentucky Transportation Cabinet; Mark Woods and Kelly Hoeksema from the National Park Service; and Nick Melton, Mike Jones, and John Burke from the Cumberland Gap Tunnel Authority. We also thank Audrey Sawyer for reviewing this report.

References Cited

Bhate Engineering Corp.–Transportation Division, 1992, Geologic mapping final report: Cumberland Gap Tunnel Project, v. II, Peripheral geologic maps, 25 p.

Burak, R.J., 2004, Permeable interlocking concrete pavements—Selection, design, construction and maintenance: Innovations in Managing Roadway Runoff to Protect Surface Water and Groundwater, 2004 Annual Conference of the Transportation Association of Canada, Quebec City, Quebec, 16 p.

Englund, K.J., 1964, Geology of the Middlesboro South quadrangle, Tennessee-Kentucky-Virginia: U.S. Geological Survey Geologic Quadrangle Map GQ-301, scale 1:24,000.

Golder Associates, 1987, The Cumberland Gap pilot tunnel and geotechnical recommendations for the main tunnels: Federal Highway Administration, Cumberland Gap Project Office, Harrogate, Tenn., v. 1 of 4, 181 p.

Harvey, R.W., and Harms, H., 2002, Tracers in groundwater: Use of microorganisms and microspheres, *in* Bitton, G., ed., Encyclopedia of environmental microbiology: New York, Wiley, v. 6, p. 3194–3202.

Parkhurst, D.L., and Appelo, C.A.J., 1999, User's guide to PHREEQC (version 2)—A computer program for speciation, batch-reaction, one-dimensional transport, and inverse geochemical calculations: U.S. Geological Survey Water-Resources Investigations Report 99-4259, 312 p.

Rister, B.W., 2005, Cumberland Gap Tunnel pavement problem: Kentucky Transportation Center Report KTC-05-35-KH5O-1F, 19 p.

Rister, B.W., 2010, Pavement settlement issues and hydrogeochemical water testing results for the Cumberland Gap Tunnel: Kentucky Transportation Center Report KTC-10-03/KH58-07-IF, 28 p.

U.S. Department of Agriculture–Soil Conservation Service, 1956?, National engineering handbook, hydraulic, section 5: U.S. Department of Agriculture, 271 p.

Vanover, J.D., 1989, Stratigraphy of pilot-tunnel through Cumberland Mountain (Kentucky-Tennessee): Richmond, Eastern Kentucky University, master's thesis, 80 p.